

Azimuthal Angle Correlations for Rapidity Separated Hadron Pairs in $d + \text{Au}$ Collisions at $\sqrt{s_{NN}} = 200 \text{ GeV}$

S. S. Adler,⁵ S. Afanasiev,²⁰ C. Aidala,¹⁰ N. N. Ajitanand,⁴⁴ Y. Akiba,^{21,40} A. Al-Jamel,³⁵ J. Alexander,⁴⁴ K. Aoki,²⁵ L. Aphecetche,⁴⁶ R. Armendariz,³⁵ S. H. Aronson,⁵ R. Averbeck,⁴⁵ T. C. Awes,³⁶ V. Babintsev,¹⁷ A. Baldisseri,¹¹ K. N. Barish,⁶ P. D. Barnes,²⁸ B. Bassalleck,³⁴ S. Bathe,^{6,31} S. Batsouli,¹⁰ V. Baublis,³⁹ F. Bauer,⁶ A. Bazilevsky,^{5,41} S. Belikov,^{19,17} M. T. Bjornrdal,¹⁰ J. G. Boissevain,²⁸ H. Borel,¹¹ M. L. Brooks,²⁸ D. S. Brown,³⁵ N. Bruner,³⁴ D. Bucher,³¹ H. Buesching,^{5,31} V. Bumazhnov,¹⁷ G. Bunce,^{5,41} J. M. Burward-Hoy,^{28,27} S. Butsyk,⁴⁵ X. Camard,⁴⁶ P. Chand,⁴ W. C. Chang,² S. Chernichenko,¹⁷ C. Y. Chi,¹⁰ J. Chiba,²¹ M. Chiu,¹⁰ I. J. Choi,⁵³ R. K. Choudhury,⁴ T. Chujo,⁵ V. Cianciolo,³⁶ Y. Cobigo,¹¹ B. A. Cole,¹⁰ M. P. Comets,³⁷ P. Constantin,¹⁹ M. Csanád,¹³ T. Csörgő,²² J. P. Cussonneau,⁴⁶ D. d'Enterria,¹⁰ K. Das,¹⁴ G. David,⁵ F. Deák,¹³ H. Delagrange,⁴⁶ A. Denisov,¹⁷ A. Deshpande,⁴¹ E. J. Desmond,⁵ A. Devismes,⁴⁵ O. Dietzsch,⁴² J. L. Drachenberg,¹ O. Drapier,²⁶ A. Drees,⁴⁵ A. Durum,¹⁷ D. Dutta,⁴ V. Dzhordzhadze,⁴⁷ Y. V. Efremenko,³⁶ H. En'yo,^{40,41} B. Espagnon,³⁷ S. Esumi,⁴⁹ D. E. Fields,^{34,41} C. Finck,⁴⁶ F. Fleuret,²⁶ S. L. Fokin,²⁴ B. D. Fox,⁴¹ Z. Fraenkel,⁵² J. E. Frantz,¹⁰ A. Franz,⁵ A. D. Frawley,¹⁴ Y. Fukao,^{25,40,41} S.-Y. Fung,⁶ S. Gadrat,²⁹ M. Germain,⁴⁶ A. Glenn,⁴⁷ M. Gonin,²⁶ J. Gosset,¹¹ Y. Goto,^{40,41} R. Granier de Cassagnac,²⁶ N. Grau,¹⁹ S. V. Greene,⁵⁰ M. Grosse Perdekamp,^{18,41} H.-Å. Gustafsson,³⁰ T. Hachiya,¹⁶ J. S. Haggerty,⁵ H. Hamagaki,⁸ A. G. Hansen,²⁸ E. P. Hartouni,²⁷ M. Harvey,⁵ K. Hasuko,⁴⁰ R. Hayano,⁸ X. He,¹⁵ M. Heffner,²⁷ T. K. Hemmick,⁴⁵ J. M. Heuser,⁴⁰ P. Hidas,²² H. Hiejima,¹⁸ J. C. Hill,¹⁹ R. Hobbs,³⁴ W. Holzmann,⁴⁴ K. Homma,¹⁶ B. Hong,²³ A. Hoover,³⁵ T. Horaguchi,^{40,41,48} T. Ichihara,^{40,41} V. V. Ikonnikov,²⁴ K. Imai,^{25,40} M. Inaba,⁴⁹ M. Inuzuka,⁸ D. Isenhower,¹ L. Isenhower,¹ M. Ishihara,⁴⁰ M. Issah,⁴⁴ A. Isupov,²⁰ B. V. Jacak,⁴⁵ J. Jia,⁴⁵ O. Jinnouchi,^{40,41} B. M. Johnson,⁵ S. C. Johnson,²⁷ K. S. Joo,³² D. Jouan,³⁷ F. Kajihara,⁸ S. Kametani,^{8,51} N. Kamihara,^{40,48} M. Kaneta,⁴¹ J. H. Kang,⁵³ K. Katou,⁵¹ T. Kawabata,⁸ A. V. Kazantsev,²⁴ S. Kelly,^{9,10} B. Khachaturov,⁵² A. Khanzadeev,³⁹ J. Kikuchi,⁵¹ D. J. Kim,⁵³ E. Kim,⁴³ G.-B. Kim,²⁶ H. J. Kim,⁵³ E. Kinney,⁹ A. Kiss,¹³ E. Kistenev,⁵ A. Kiyomichi,⁴⁰ C. Klein-Boesing,³¹ H. Kobayashi,⁴¹ L. Kochenda,³⁹ V. Kochetkov,¹⁷ R. Kohara,¹⁶ B. Komkov,³⁹ M. Konno,⁴⁹ D. Kotchetkov,⁶ A. Kozlov,⁵² P. J. Kroon,⁵ C. H. Kuberg,^{1,*} G. J. Kunde,²⁸ K. Kurita,⁴⁰ M. J. Kweon,²³ Y. Kwon,⁵³ G. S. Kyle,³⁵ R. Lacey,⁴⁴ J. G. Lajoie,¹⁹ Y. Le Bornec,³⁷ A. Lebedev,^{19,24} S. Leckey,⁴⁵ D. M. Lee,²⁸ M. J. Leitch,²⁸ M. A. L. Leite,⁴² X. H. Li,⁶ H. Lim,⁴³ A. Litvinenko,²⁰ M. X. Liu,²⁸ C. F. Maguire,⁵⁰ Y. I. Makdisi,⁵ A. Malakhov,²⁰ V. I. Manko,²⁴ Y. Mao,^{38,40} G. Martinez,⁴⁶ H. Masui,⁴⁹ F. Matathias,⁴⁵ T. Matsumoto,^{8,51} M. C. McCain,¹ P. L. McGaughey,²⁸ Y. Miake,⁴⁹ T. E. Miller,⁵⁰ A. Milov,⁴⁵ S. Mioduszewski,⁵ G. C. Mishra,¹⁵ J. T. Mitchell,⁵ A. K. Mohanty,⁴ D. P. Morrison,⁵ J. M. Moss,²⁸ D. Mukhopadhyay,⁵² M. Muniruzzaman,⁶ S. Nagamiya,²¹ J. L. Nagle,^{9,10} T. Nakamura,¹⁶ J. Newby,⁴⁷ A. S. Nyanin,²⁴ J. Nystrand,³⁰ E. O'Brien,⁵ C. A. Ogilvie,¹⁹ H. Ohnishi,⁴⁰ I. D. Ojha,^{3,50} H. Okada,^{25,40} K. Okada,^{40,41} A. Oskarsson,³⁰ I. Otterlund,³⁰ K. Oyama,⁸ K. Ozawa,⁸ D. Pal,⁵² A. P. T. Palounek,²⁸ V. Pantuev,⁴⁵ V. Papavassiliou,³⁵ J. Park,⁴³ W. J. Park,²³ S. F. Pate,³⁵ H. Pei,¹⁹ V. Penev,²⁰ J.-C. Peng,¹⁸ H. Pereira,¹¹ V. Peresedov,²⁰ A. Pierson,³⁴ C. Pinkenburg,⁵ R. P. Pisani,⁵ M. L. Purschke,⁵ A. K. Purwar,⁴⁵ J. M. Qualls,¹ J. Rak,¹⁹ I. Ravinovich,⁵² K. F. Read,^{36,47} M. Reuter,⁴⁵ K. Reygers,³¹ V. Riabov,³⁹ Y. Riabov,³⁹ G. Roche,²⁹ A. Romana,^{26,*} M. Rosati,¹⁹ S. S. E. Rosendahl,³⁰ P. Rosnet,²⁹ V. L. Rykov,⁴⁰ S. S. Ryu,⁵³ N. Saito,^{25,40,41} T. Sakaguchi,^{8,51} S. Sakai,⁴⁹ V. Samsonov,³⁹ L. Sanfratello,³⁴ R. Santo,³¹ H. D. Sato,^{25,40} S. Sato,^{5,49} S. Sawada,²¹ Y. Schutz,⁴⁶ V. Semenov,¹⁷ R. Seto,⁶ T. K. Shea,⁵ I. Shein,¹⁷ T.-A. Shibata,^{40,48} K. Shigaki,¹⁶ M. Shimomura,⁴⁹ A. Sickles,⁴⁵ C. L. Silva,⁴² D. Silvermyr,²⁸ K. S. Sim,²³ A. Soldatov,¹⁷ R. A. Soltz,²⁷ W. E. Sondheim,²⁸ S. P. Sorensen,⁴⁷ I. V. Sourikova,⁵ F. Staley,¹¹ P. W. Stankus,³⁶ E. Stenlund,³⁰ M. Stepanov,³⁵ A. Ster,²² S. P. Stoll,⁵ T. Sugitate,¹⁶ J. P. Sullivan,²⁸ S. Takagi,⁴⁹ E. M. Takagui,⁴² A. Taketani,^{40,41} K. H. Tanaka,²¹ Y. Tanaka,³³ K. Tanida,⁴⁰ M. J. Tannenbaum,⁵ A. Taranenko,⁴⁴ P. Tarján,¹² T. L. Thomas,³⁴ M. Togawa,^{25,40} J. Tojo,⁴⁰ H. Torii,^{25,41} R. S. Towell,¹ V.-N. Tram,²⁶ I. Tserruya,⁵² Y. Tsuchimoto,¹⁶ H. Tydesjö,³⁰ N. Tyurin,¹⁷ T. J. Uam,³² H. W. van Hecke,²⁸ J. Velkovska,⁵ M. Velkovsky,⁴⁵ V. Veszprémi,¹² A. A. Vinogradov,²⁴ M. A. Volkov,²⁴ E. Vznuzdaev,³⁹ X. R. Wang,¹⁵ Y. Watanabe,^{40,41} S. N. White,⁵ N. Willis,³⁷ F. K. Wohn,¹⁹ C. L. Woody,⁵ W. Xie,⁶ A. Yanovich,¹⁷ S. Yokkaichi,^{40,41} G. R. Young,³⁶ I. E. Yushmanov,²⁴ W. A. Zajc,^{10,†} C. Zhang,¹⁰ S. Zhou,⁷ J. Zimányi,²² L. Zolin,²⁰ and X. Zong¹⁹

(PHENIX Collaboration)

¹Abilene Christian University, Abilene, Texas 79699, USA

²Institute of Physics, Academia Sinica, Taipei 11529, Taiwan

- ³Department of Physics, Banaras Hindu University, Varanasi 221005, India
⁴Bhabha Atomic Research Centre, Bombay 400 085, India
⁵Brookhaven National Laboratory, Upton, New York 11973-5000, USA
⁶University of California-Riverside, Riverside, California 92521, USA
⁷China Institute of Atomic Energy (CIAE), Beijing, People's Republic of China
⁸Center for Nuclear Study, Graduate School of Science, University of Tokyo, 7-3-1 Hongo, Bunkyo, Tokyo 113-0033, Japan
⁹University of Colorado, Boulder, Colorado 80309, USA
¹⁰Columbia University, New York, New York 10027, and Nevis Laboratories, Irvington, New York 10533, USA
¹¹Dapnia, CEA Saclay, F-91191, Gif-sur-Yvette, France
¹²Debrecen University, H-4010 Debrecen, Egyetem tér 1, Hungary
¹³ELTE, Eötvös Loránd University, H - 1117 Budapest, Pázmány P. s. 1/A, Hungary
¹⁴Florida State University, Tallahassee, Florida 32306, USA
¹⁵Georgia State University, Atlanta, Georgia 30303, USA
¹⁶Hiroshima University, Kagamiyama, Higashi-Hiroshima 739-8526, Japan
¹⁷IHEP Protvino, State Research Center of Russian Federation, Institute for High Energy Physics, Protvino, 142281, Russia
¹⁸University of Illinois at Urbana-Champaign, Urbana, Illinois 61801, USA
¹⁹Iowa State University, Ames, Iowa 50011, USA
²⁰Joint Institute for Nuclear Research, 141980 Dubna, Moscow Region, Russia
²¹KEK, High Energy Accelerator Research Organization, Tsukuba, Ibaraki 305-0801, Japan
²²KFKI Research Institute for Particle and Nuclear Physics of the Hungarian Academy of Sciences (MTA KFKI RMKI), H-1525 Budapest 114, POBox 49, Budapest, Hungary
²³Korea University, Seoul, 136-701, Korea
²⁴Russian Research Center "Kurchatov Institute", Moscow, Russia
²⁵Kyoto University, Kyoto 606-8502, Japan
²⁶Laboratoire Leprince-Ringuet, Ecole Polytechnique, CNRS-IN2P3, Route de Saclay, F-91128, Palaiseau, France
²⁷Lawrence Livermore National Laboratory, Livermore, California 94550, USA
²⁸Los Alamos National Laboratory, Los Alamos, New Mexico 87545, USA
²⁹LPC, Université Blaise Pascal, CNRS-IN2P3, Clermont-Fd, 63177 Aubiere Cedex, France
³⁰Department of Physics, Lund University, Box 118, SE-221 00 Lund, Sweden
³¹Institut für Kernphysik, University of Muenster, D-48149 Muenster, Germany
³²Myongji University, Yongin, Kyonggido 449-728, Korea
³³Nagasaki Institute of Applied Science, Nagasaki-shi, Nagasaki 851-0193, Japan
³⁴University of New Mexico, Albuquerque, New Mexico 87131, USA
³⁵New Mexico State University, Las Cruces, New Mexico 88003, U.S., USA
³⁶Oak Ridge National Laboratory, Oak Ridge, Tennessee 37831, USA
³⁷IPN-Orsay, Université Paris Sud, CNRS-IN2P3, BP1, F-91406, Orsay, France
³⁸Peking University, Beijing, People's Republic of China
³⁹PNPI, Petersburg Nuclear Physics Institute, Gatchina, Leningrad region, 188300, Russia
⁴⁰RIKEN (The Institute of Physical and Chemical Research), Wako, Saitama 351-0198, Japan
⁴¹RIKEN BNL Research Center, Brookhaven National Laboratory, Upton, New York 11973-5000, USA
⁴²Universidade de São Paulo, Instituto de Física, Caixa Postal 66318, São Paulo CEP05315-970, Brazil
⁴³System Electronics Laboratory, Seoul National University, Seoul, South Korea
⁴⁴Chemistry Department, Stony Brook University, SUNY, Stony Brook, New York 11794-3400, USA
⁴⁵Department of Physics and Astronomy, Stony Brook University, SUNY, Stony Brook, New York 11794, USA
⁴⁶SUBATECH (Ecole des Mines de Nantes, CNRS-IN2P3, Université de Nantes), BP 20722 - 44307, Nantes, France
⁴⁷University of Tennessee, Knoxville, Tennessee 37996, USA
⁴⁸Department of Physics, Tokyo Institute of Technology, Oh-okayama, Meguro, Tokyo 152-8551, Japan
⁴⁹Institute of Physics, University of Tsukuba, Tsukuba, Ibaraki 305, Japan
⁵⁰Vanderbilt University, Nashville, Tennessee 37235, USA
⁵¹Advanced Research Institute for Science and Engineering, Waseda University, 17 Kikui-cho, Shinjuku-ku, Tokyo 162-0044, Japan
⁵²Weizmann Institute, Rehovot 76100, Israel
⁵³Yonsei University, IPAP, Seoul 120-749, Korea

(Received 17 March 2006; published 8 June 2006)

Deuteron-gold ($d + \text{Au}$) collisions at the Relativistic Heavy Ion Collider provide ideal platforms for testing QCD theories in dense nuclear matter at high energy. In particular, models suggesting strong saturation effects for partons carrying small nucleon momentum fraction (x) predict modifications to jet production at forward rapidity (deuteron-going direction) in $d + \text{Au}$ collisions. We report on two-particle azimuthal angle correlations between charged hadrons at forward/backward (deuteron/gold going direction) rapidity and charged hadrons at midrapidity in $d + \text{Au}$ and $p + p$ collisions at $\sqrt{s_{NN}} = 200$ GeV. Jet structures observed in the correlations are quantified in terms of the conditional yield and angular

width of away-side partners. The kinematic region studied here samples partons in the gold nucleus with $x \sim 0.1$ to ~ 0.01 . Within this range, we find no x dependence of the jet structure in $d + \text{Au}$ collisions.

DOI: [10.1103/PhysRevLett.96.222301](https://doi.org/10.1103/PhysRevLett.96.222301)

PACS numbers: 25.75.Dw, 25.75.Gz

Observations in $d + \text{Au}$ collisions at $\sqrt{s_{NN}} = 200$ GeV at the Relativistic Heavy Ion Collider (RHIC) reveal a significant suppression of hadron production at forward rapidity (deuteron-going direction) relative to $p + p$ collisions scaled up by the equivalent number of nucleon-nucleon collisions (N_{coll}) [1–3]. This suppression is observed for hadrons with momentum transverse to the beam direction in the range $p_T \approx 1.5\text{--}4$ GeV/ c . In contrast, measurements at midrapidity [4–7] and backward rapidity [1–3] show a modest enhancement relative to N_{coll} scaling in the same p_T range. Particle production at forward rapidity is sensitive to partons in the gold nucleus which carry a small nucleon momentum fraction (small Bjorken x). The suppression has generated significant theoretical interest including different calculational frameworks for understanding the data [8–11].

One such framework, the color glass condensate (CGC), attempts to describe the data in terms of gluon saturation [8]. At small x the probability of emitting an extra gluon is large and the number of gluons grows in a limited transverse area. When the transverse density becomes large, partons start to overlap and gluon-gluon fusion processes start to dominate the parton evolution in the hadronic wave functions. Thus the gluon density saturates. Since the non-linear growth of the gluon density depends on the transverse size of the system, gluon saturation effects are expected to set in at higher x for heavy nuclei than for free nucleons.

In the leading order pQCD framework, a quark or gluon jet with large transverse momentum produced in a hard-scattering process (high momentum transfer or large Q^2) must be momentum balanced by another quark or gluon jet in the opposite direction but with almost the same p_T . Thus the azimuthal angle correlation between particles from the pair of jets (referred to as dijets) is characterized by two peak structures separated by 180° . In CGC calculations, the momentum to balance a jet may come from a large multiplicity of gluons in the saturation regime, and thus no single partner jet may appear on the opposite side [12]. This effect is analogous to the nuclear Mössbauer effect, and is often referred to as the appearance of monojets. Alternative calculations, describing the suppression of single hadrons at forward rapidity in $d + \text{Au}$ reactions in terms of leading twist pQCD effects, predict no such monojet feature [13].

We want to probe this high gluon density regime in $d + \text{Au}$ collisions with relatively high p_T particles at forward rapidity. Such particles are likely to result from hard-scattering collisions involving small x partons in the gold nucleus. At small x the gluon density increases rapidly with

Q^2 and saturation effects may be relevant for $x \approx 0.01$ at modest p_T . CGC calculations [12] predict significant suppression of the conditional yield and widening of away-side jet azimuthal correlations between rapidity-separated hadron pairs when one of those hadrons is at forward rapidity.

In this Letter we report on measurements of two-particle azimuthal angle correlations between unidentified charged hadrons in $p + p$ and $d + \text{Au}$ collisions at $\sqrt{s_{NN}} = 200$ GeV. In our analysis, the two particles are referred to as the *trigger* and *associated* particles. The trigger particle is at forward ($1.4 < \eta < 2.0$) or backward ($-2.0 < \eta < -1.4$) rapidity and the associated particle is at midrapidity, $|\eta| < 0.35$. The particles are separated by an average pseudorapidity gap $\langle \Delta\eta \rangle \sim 1.5$. The criteria for trigger particles, associated particles, and event selection are described elsewhere [3,14]. The two-particle azimuthal angle correlation technique has been used extensively by RHIC experiments and is described in detail elsewhere [14–18]. In this technique the azimuthal correlation function is formed from the angular difference, $\Delta\phi = \phi^{\text{assoc}} - \phi^{\text{trig}}$, between each trigger and associated particle pair. Two jet peaks are normally observed in such correlation functions: the near-side peak ($\Delta\phi \sim 0$) in which the two particles come from the same jet, and the away-side peak ($\Delta\phi \sim \pi$) in which they come from back-to-back jets. In addition to these peaks the correlation functions also have a $\Delta\phi$ independent combinatoric background contribution due to trigger-associated pairs from different jets or from non-jet processes.

We can construct separate correlation functions that are sensitive to partons in the gold nucleus with different x ranges. By choosing trigger particles with $1.0 < p_T < 5.0$ GeV/ c at forward (backward) rapidity and associated particles with $0.5 < p_T < 2.5$ GeV/ c at midrapidity, we sample partons in gold nuclei with $x \sim 0.01(0.1)$. We do not expect our data at $x \sim 0.1$ to be sensitive to saturation effects, but they may at $x \sim 0.01$ [19]. The comparison in $d + \text{Au}$ reactions between these two cases, as well as with the $p + p$ case, may give insights into possible saturation effects on jet production and other mechanisms for forward rapidity single-particle suppression. It should be noted that the prediction of monojets in [12] assumes one particle at $\eta = 3.8$ and one at midrapidity, thus demonstrating sensitivity at smaller x ($\sim 10^{-4}$) than presented in this analysis.

Data for this analysis were collected by PHENIX [20] in 2003. For $d + \text{Au}$ collisions, we divide the data into two centrality (impact parameter) classes based on the number of hits in the backward-rapidity PHENIX beam-beam counter (BBC, $-3.9 < \eta < -3.0$). Central (peripheral)

collisions comprise 0%–40% (40%–88%) of the minimum bias cross section. Using a Glauber model [3] and a simulation of the BBC, we determine $\langle N_{\text{coll}} \rangle = 13.0 \pm 0.9 (4.7 \pm 0.4)$ for central (peripheral) collisions.

Trigger particles are unidentified charged hadrons measured in the PHENIX muon spectrometers [20]. We only select particles from $1.4 < |\eta| < 2.0$ to obtain homogeneous acceptance from $1 < p_T < 5$ GeV/c and to reduce beam correlated backgrounds. We identify hadrons, as opposed to muons, in the muon spectrometers by comparing their momentum and penetration depth [3]. It is notable that our trigger hadrons have a modified composition (pion/kaon/proton ratio) relative to that at the collision vertex due to species-dependent nuclear interaction cross sections. Detailed simulations show that kaons make up 65%–90% of positively charged trigger particles and pions make up 70%–90% of negatively charged trigger particles. The sizes of the quoted ranges of particle composition are due to uncertainties on the input particle compositions in simulation and due to variations, correlated with polar angle and therefore rapidity, in the length of absorber material that particles traverse. The baryon contribution to our trigger particle sample is negligible. We find the two-particle azimuthal angle correlations for positively and negatively charged trigger particles to be consistent and therefore combined the results. Associated particles are unidentified charged hadrons measured in the PHENIX central spectrometers [20] which cover $|\eta| < 0.35$ and in this analysis have $0.5 < p_T < 2.5$ GeV/c. Standard track selection criteria [14] are applied.

For comparison we have also included measurements where trigger particles and associated particles are both measured in the PHENIX central spectrometers at midrapidity. The $d + \text{Au}$ points for this comparison are from [14] and the $p + p$ point is an extension in p_T of the analysis that was published in [16].

We define the azimuthal angle correlation function as $\text{CF} = \frac{dN(\Delta\phi)/d(\Delta\phi)}{\text{acc}(\Delta\phi)}$, where $dN(\Delta\phi)/d(\Delta\phi)$ is the measured two-particle distribution and $\text{acc}(\Delta\phi)$ is the two-particle acceptance obtained by mixing trigger particles and associated particles from different events within the same centrality and collision vertex category. This correction is necessary because the PHENIX central arm detector is not azimuthally symmetric and the pair acceptance varies as a function of $\Delta\phi$.

Figure 1 shows the correlation functions for trigger particles with $p_T = 2\text{--}5$ GeV/c and associated particles with $p_T = 0.5\text{--}1.0$ GeV/c. A clear peak is seen near $\Delta\phi = \pi$ on all plots corresponding to the away-side jet. It is notable that there is no peak near $\Delta\phi = 0$, as expected, because the rapidity gap between the two particles is larger than the width of the near-side jet. Although the rapidity of away-side particles is not necessarily the same as the rapidity of the away-side jet, PYTHIA [21] studies show that the distribution of final state particles around the

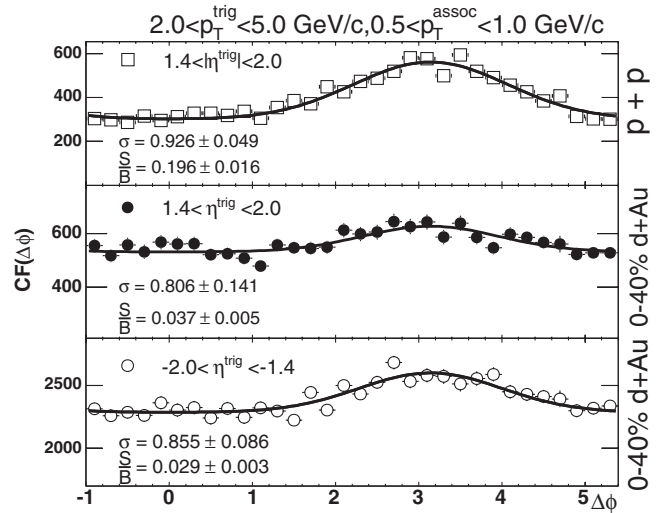


FIG. 1. Azimuthal angle correlation functions. Gaussian widths from the fits and the signal to background ratio integrated over $\pi - 1 < \Delta\phi < \pi + 1$ are shown. Note that the y axis is zero suppressed on the middle and bottom panels.

jet axis is symmetric in $\Delta\eta$ and $\Delta\phi$ and the jet cone width is less than 1 unit of rapidity, which is smaller than the rapidity gap.

After constructing the correlation functions in various bins in p_T^{assoc} , p_T^{trig} , and η^{trig} we used two methods to determine the unnormalized number of trigger-associated particle pairs, N_{pair} , above a constant background. In the first method, we define $N_{\text{pair}} = \sum_{\Delta\phi=\pi-1}^{\pi+1} \text{CF}(\Delta\phi) - \sum_{\Delta\phi=-1}^{\pi+1} \text{CF}(\Delta\phi)$, where the first term is the integral of the correlation function (CF) in the area of the correlation peak ($\pi - 1 < \Delta\phi < \pi + 1$) and the second term is the integral away from the peak ($-1 < \Delta\phi < 1$). In the second method we fit the correlation function with a Gaussian distribution centered at $\Delta\phi = \pi$ plus a constant background. The values of N_{pair} obtained by both methods are found to be consistent and the small differences are included in our systematic errors. The solid lines in Fig. 1 show the resulting fits. Gaussian width parameters (σ) and the integrated signal to background ratios ($\frac{S}{B}$) over the signal region ($\pi - 1 < \Delta\phi < \pi + 1$) are quoted.

The conditional yield (CY) (per trigger particle) is defined to be $\text{CY} = \frac{N_{\text{pair}}/\epsilon_{\text{assoc}}}{N_{\text{trig}}}$, where ϵ_{assoc} ($\sim 0.15 \pm 0.015$) is the efficiency times acceptance for associated particles and N_{trig} is the number of trigger particles used to generate the correlation function. ϵ_{assoc} is obtained for each colliding system, centrality class, and p_T bin by a GEANT based simulation of the PHENIX detector [14].

It is interesting to plot the conditional yields as a function of η^{trig} . Changing η^{trig} from -2.0 to 2.0 effectively changes the range of Bjorken x of sampled partons in gold nuclei from $0.1_{-0.04}^{+0.06}$ to $0.01_{-0.007}^{+0.02}$. Figure 2 shows the

results. The first observation is that there is no difference beyond statistical fluctuations in the conditional yields for $p + p$, $d + \text{Au}$ peripheral, or $d + \text{Au}$ central collisions at any trigger particle pseudorapidity.

We further quantify any nuclear modification in the conditional yield by defining a ratio $I_{d\text{Au}} = \frac{\text{CY}_{d+\text{Au}}}{\text{CY}_{p+p}}$. The technique of comparing conditional yields per trigger to investigate the source of single-particle nuclear modifications in the trigger particle region of phase space is well established at RHIC [14–16]. The fact that single-particle yields are strongly modified in the trigger particle p_T range makes $I_{d\text{Au}}$ particularly interesting since it may shed light on the nature of the single-particle suppression. For our rapidity-separated pairs two different models [12,13], which posit different mechanisms to be responsible for the single-particle suppression, predict very different results for the evolution of the correlation function vs centrality and x .

Figure 3 shows the ratio $I_{d\text{Au}}$ vs p_T^{assoc} for different p_T^{trig} , η^{trig} and $d + \text{Au}$ centrality bins. Shaded bands on each data point show point-to-point independent systematic errors due to differences in N_{pair} obtained from the two methods described above. There is also a point-to-point correlated $\sim 2\%$ systematic uncertainty in the centrality dependence of $\varepsilon_{\text{assoc}}$ determined by embedding Monte Carlo tracks into real events. The size of this uncertainty is comparable to the width of the $I_{d\text{Au}} = 1$ line.

For trigger particles at both forward rapidity (sampling low- x partons in the gold nucleus) and backward rapidity (sampling high- x partons in the gold nucleus), the measured $I_{d\text{Au}}$ is consistent with one. There may even be some

evidence of slight enhancement for the case with trigger particles at forward rapidity in central $d + \text{Au}$ collisions. We note that if monojets were a major contributor to the trigger particle sample in our x range, we would have expected a decrease in the conditional yield for $d + \text{Au}$ central collisions with the trigger particle at forward rapidity.

Our measurement is inconsistent with any large nuclear suppression (i.e., monojets) of the jet structure in this kinematic range, but it is in agreement with leading twist pQCD calculations that predict suppression of single-particle yields at forward rapidity, with little modification of the conditional yield [13]. However, we note that in these modest p_T ranges, there may be contributions from both “hard” (large Q^2) processes and “soft” coherent (small Q^2) processes. In $d + \text{Au}$ collisions soft particle production is shifted backwards in rapidity [22]. Thus, the fraction of hadrons at forward rapidity from hard processes may be increased in central $d + \text{Au}$ reactions. This may offer an explanation for the modest enhancement seen in the conditional yield for this case and could also mask a small monojet signal.

We have also compared the Gaussian widths of the correlation peaks in $d + \text{Au}$ collisions vs $p + p$ collisions. Ratios of the $d + \text{Au}$ to $p + p$ widths are plotted in Fig. 4 vs p_T^{assoc} . There may be a hint of a slight p_T^{assoc} dependence in the ratio, but overall there is no significant difference in the width in $d + \text{Au}$ collisions for different η^{trig} .

In conclusion, we measured two-particle azimuthal correlations with trigger particles at forward, backward, and midrapidity and correlated them with associated particles at midrapidity in $d + \text{Au}$ and $p + p$ collisions. Associated particle conditional yields in central $d + \text{Au}$ collisions are consistent with those in $p + p$ collisions and are consistent over the range $|\eta^{\text{trig}}| < 2.0$. We have also compared the widths of the away-side jet peaks in $d + \text{Au}$ and $p + p$ collisions, and find no evidence for η^{trig} -dependent modification within our statistical errors. Overall the results

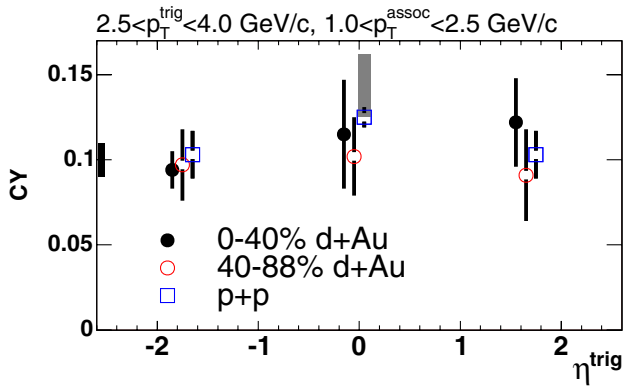


FIG. 2 (color online). Conditional yields are shown as a function of trigger particle pseudorapidity. Data points at midrapidity for $d + \text{Au}$ collisions are from [14]. To increase visibility, we artificially shift data points belonging to the same η^{trig} bin. The errors on each point are statistical. The black bar around 0.1 on the y axis indicates a 10% common systematic error for all the data points due to uncertainties in $\varepsilon_{\text{assoc}}$. There is an additional +0.037 systematic error on the midrapidity $p + p$ point from jet yield extraction, which is shown as the gray bar on that point (similar analysis as [16]).

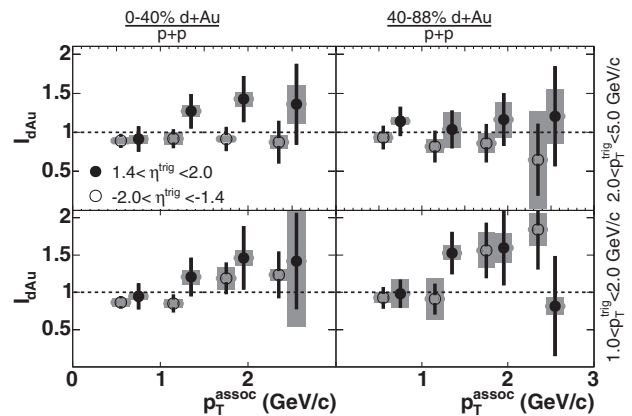


FIG. 3. $I_{d\text{Au}}$ vs p_T^{assoc} for different centrality, p_T^{trig} and η^{trig} bins. To increase visibility, we artificially shift data points belonging to the same p_T^{assoc} bin.

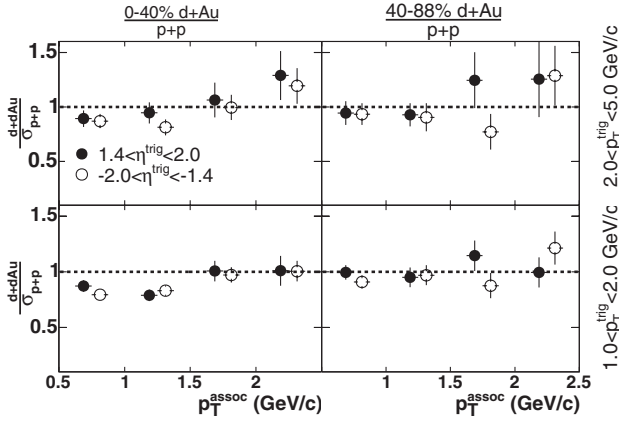


FIG. 4. The ratio of correlation peak widths between $d + Au$ and $p + p$ collisions. Only statistical errors are shown. To increase visibility, we artificially shift the data points belonging to the same p_T^{assoc} bin.

presented here do not support models that predict strong modifications on jet production in the kinematic range covered by this analysis. However, we also note that the backwards rapidity shift of soft particle production may reduce the amplitude of such modifications.

We thank the staff of the Collider-Accelerator and Physics Departments at BNL for their vital contributions. We acknowledge support from the Department of Energy and NSF (U.S.A.), MEXT, and JSPS (Japan), CNPq and FAPESP (Brazil), NSFC (China), IN2P3/CNRS, CEA, and ARMINES (France), BMBF, DAAD, and AvH (Germany), OTKA (Hungary), DAE and DST (India), ISF (Israel), KRF and CHEP (Korea), RMIST, RAS, and RMAE (Russia), VR and KAW (Sweden), U.S. CRDF for the

FSU, US-Hungarian NSF-OTKA-MTA, and US-Israel BSF.

*Deceased.

†PHENIX Spokesperson.

Electronic address: zajc@nevis.columbia.edu

- [1] I. Arsene *et al.*, Phys. Rev. Lett. **93**, 242303 (2004).
- [2] J. Adams *et al.*, Phys. Rev. C **70**, 064907 (2004).
- [3] S. S. Adler *et al.*, Phys. Rev. Lett. **94**, 082302 (2005).
- [4] S. S. Adler *et al.*, Phys. Rev. Lett. **91**, 072303 (2003).
- [5] J. Adams *et al.*, Phys. Rev. Lett. **91**, 072304 (2003).
- [6] B. B. Back *et al.*, Phys. Rev. Lett. **91**, 072302 (2003).
- [7] I. Arsene *et al.*, Phys. Rev. Lett. **91**, 072305 (2003).
- [8] L. McLerran and R. Venugopalan, Phys. Rev. D **49**, 2233 (1994); Phys. Rev. D **49**, 3352 (1994).
- [9] R. Vogt, Phys. Rev. C **70**, 064902 (2004).
- [10] J. Qiu and I. Vitev, hep-ph/0410218.
- [11] R. C. Hwa, C. B. Yang, and R. J. Fries, Phys. Rev. C **71**, 024902 (2005).
- [12] D. Kharzeev, E. Levin, and L. McLerran, Nucl. Phys. **A748**, 627 (2005).
- [13] J. Qiu and I. Vitev, Phys. Lett. B **632**, 507 (2006).
- [14] S. S. Adler *et al.*, nucl-ex/0510021.
- [15] C. Adler *et al.*, Phys. Rev. Lett. **90**, 082302 (2003).
- [16] S. S. Adler *et al.*, Phys. Rev. C **71**, 051902(R) (2005).
- [17] J. Adams *et al.*, Phys. Rev. Lett. **95**, 152301 (2005).
- [18] S. S. Adler *et al.*, nucl-ex/0507004.
- [19] M. Arneodo, Phys. Rep. **240**, 301 (1994).
- [20] K. Adcox *et al.*, Nucl. Instrum. Methods Phys. Res., Sect. A **499**, 469 (2003).
- [21] T. Sjostrand *et al.*, Comput. Phys. Commun. **135**, 238 (2001).
- [22] B. B. Back *et al.*, Phys. Rev. C **72**, 031901 (2005).